Measurement of $W^{\pm}$ single spin asymmetries and W cross section ratio in polarized $p+p$ collisions at $\sqrt{s} = 510$ GeV at STAR

Devika Gunarathne*
Temple University

(for the STAR collaboration)
(Dated: December 27, 2016)

We present the preliminary results of measurements of single spin asymmetries, A_L for $W^{\pm}$ boson production in longitudinally polarized p+p collisions at $\sqrt{s} = 510$ GeV and measurements of cross section ratio, $\sigma_{W^+}/\sigma_{W^-}$, for W^+, W^- boson production in p+p collisions at $\sqrt{s} = 500$ and 510 GeV. The asymmetry measurements are based on 246.2 pb^{-1} of data taken in the RHIC 2013 run and the cross section ratio measurements are based on 102 pb^{-1} of data taken during RHIC 2011 and 2012 runs by the STAR experiment. The both results are shown as a function of the decay lepton pseudorapidity, η_e in the mid rapidity region ($|\eta_e| < 1$). At these kinematics, $W^{\pm}$ single spin asymmetries provides a theoretically clean probe of the proton's polarized quark and antiquark distributions and the W cross section ratio measurements provide sensitivity to unpolarized sea quark distributions at the scale of the W mass. The asymmetry results are consistent with the recently published STAR $A_L^{W^{\pm}}$ results based on data collected during RHIC 2011 and 2012 runs which showed a preference for a sizable, positive up antiquark polarization in the range $0.05 < x < 0.2$. The new preliminary results can be considered as the most precise results of $A_L^{W^{\pm}}$ in the world to the date, with uncertainty reduced by 40% in comparison to the published results. Both asymmetry results and cross section ratio results agree with theoretical predictions, constrained by polarized DIS and recent unpolarized parton distribution functions respectively.

I. INTRODUCTION

There has been steady progress over the past few decades in terms of understanding the spin structure of the nucleon, one of the fundamental questions in nuclear physics. In the 1980s, the spin of the proton was naively explained [1] by the alignment of spins of the valence quarks. However, in our current understanding [2] , the valence quarks, sea quarks, gluons and their possible orbital angular momentum are all expected to contribute to the overall spin of the proton. Despite this significant progress, our understanding of the individual polarizations of quarks and antiquarks is not yet complete.

According to the spin sum rule introduced by Jaffe and Monahar [3] in 1990, the spin of the proton can be written in terms of its contributions from the intrinsic quark and antiquark polarizations, intrinsic gluon polarization and their possible orbital angular momentum. Polarized inclusive deep-inelastic scattering (DIS) experiments were able to strongly constrain the total quark contribution to the proton spin [4]. However, DIS experiments were not sensitive to the flavor separated individual quark spin contributions. These were then measured by polarized semi inclusive DIS experiments (SIDIS), where a certain hadron is tag in the final state. The helicity-dependent parton distribution functions (PDF) [4] are extracted from global analysis using the world data of both DIS and SIDIS. Relatively large uncertainties were observed in the polarized antiquark PDFs in comparisons to quark PDFs mainly due to the large uncertainties found in the fragmentation functions [13] which were used in the global analysis for SIDIS data. Over the years however, progressively more precise polarized SIDIS data, covering an enhanced kinematic range has become available [5][6][7]. Moreover the knowledge of the fragmentation process of SIDIS has increased, leading to extraction of rather precise fragmentation functions [8]. Furthermore, the global fitting tools used in various global analysis has improved over the years. Despite this significant progress in the experiments and global analysis, the current knowledge of antiquark helicity PDFs from DIS and SIDIS data are still less precise in comparison to the valence sector [21].

The production of $W^{\pm}$ bosons in longitudinally polarized $p+p$ collisions at RHIC provides an unique and powerful tool to probe the individual helicity PDFs of light quarks and anti quarks in the proton at much larger Q^2 scale ($\sim 6400\ GeV^2$) set by the W mass. Due to the maximal parity violating nature of the weak interaction, $W^{-(+)}$ bosons couple to the left handed quarks and right-handed anti quarks and hence offer direct probes of their respective helicity distributions in the nucleon. These distributions can be extracted by measuring the parity violating A_L, as a function of the decay electron (positron) pseudo rapidity, η_e. The longitudinal single-spin asymmetry is defined as $A_L = (\sigma_+ - \sigma_-)/(\sigma_+ + \sigma_-)$, where $\sigma_{+(-)}$ is the cross section when the helicity of the polarized proton beam is positive (negative). At leading order, W^+ A_L is directly related to polarized anti d and u quark distributions ($\Delta\bar{d}$, Δu) while W^- A_L is directly related to polarized anti u and d quark distributions ($\Delta\bar{u}$, Δd) [14].

Considering the SU(3) flavor symmetry, since the mass difference of up and down quarks is small, the simple perturbative picture expected to produce nearly equal numbers of up and down quark-antiquark pairs in the nucleon sea from gluon splitting. However in 1970's the first indication of up-down asymmetric sea came through early SLAC data suggesting the violation of Gottfried Sum Rule (GSR) [9]. Later on more concrete evidence supported the up-down asymmetric sea with surprising results from FNAL E866 Drell-Yan (DY) Experiment [11]. The E866 data clearly showed that $\bar{d} \neq \bar{u}$, suggesting a non perturbative origin of the nucleon sea. However, theoretical calculation failed to explain the $\bar{d}/\bar{u}$ behavior at higher Bjorken-x values [10]. Moreover, the most recent preliminary results of SeaQuest E906 [12] experiment where DY measurements have extended to larger x values deviates from E866 results at higher x values. This particular x-region where the two DY results disagrees (FNAL E866 and SeaQuest E906) and the steady increasing behavior of $\bar{d}/\bar{u}$ changes is highly sensitive to the RHIC kinematic range where W cross section ratio measurement provides an important and completely independent cross check of up-down flavor asymmetry of the sea at much larger Q^2 values than the DY measurements.

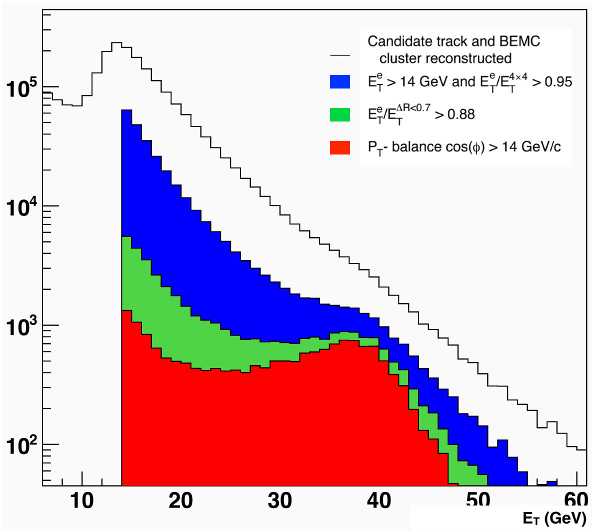

FIG. 1. Candidate E_T^e distribution from the data after various selection cuts.

This paper is organized as follows: section II provides a brief overview of the experimental aspects focusing on the use of various detector elements at STAR in terms of reconstructing and extracting W signal spectra from the data set. This section also explains the estimation and subtraction of the background from the W signal spectra. In section III we discuss the calculation of the W single spin asymmetry and W cross section ratio and present the preliminary results comparing to several theoretical calculations. Finally the last section provides a summary and outlook.

II. ANALYSIS

The data analyzed here for W A_L, is the data collected by the STAR experiment in RHIC 2013 running of longitudinally polarized $p + p$ collisions at $\sqrt{s} = 510$ GeV. The total integrated luminosity of the data is 246.2 pb^{-1}, with an average beam polarization of 54%. The data used for the W cross section analysis is the combination of data collected by the STAR experiment in RHIC 2011 and 2012 running of polarized $p + p$ collisions at $\sqrt{s} =$ 500 and 510 GeV with a total integrated luminosity of 25 pb^{-1} and 77 pb^{-1} respectively. For both analyses, the data are selected online using the same high energy trigger requirement and follows a similar procedure for reconstruction, extraction of the W signal, and estimation and subtraction of backgrounds. An additional step of correction for W detection efficiencies is involved for cross section analysis.

The STAR experiment [16] is well equipped to measure A_L for $W^{\pm}$ boson production within a pseudorapidity range of $|\eta| < 1$. $W^{\pm}$ bosons are detected via their $W^{\pm} \to e^{\pm}\nu$ decay channels. A subsystem of the STAR detector, the Time Projection Chamber (TPC) is used to measure the transverse momentum (p_T) of decay electrons and positrons and to separate their charge sign. Two other subsystems, Barrel and Endcap Electromagnetic Calorimeters (BEMC, EEMC) are used to measure the energy of decay leptons. A well developed algorithm [15] is used to identify and reconstruct $W^{\pm}$ candidate events and reducing QCD type background events. In this algorithm, various cuts are applied at each level of the selection process based on the kinematics and topological differences between the electroweak process of interest and QCD processes. For example, tracks associated with $W^{\pm}$ candidate events can be identified as isolated tracks in the TPC that point to an isolated EMC cluster in the calorimeter, where as for QCD type events have several TPC tracks point to several EMC clusters. In contrast to QCD background events, large missing transverse energy opposite in ϕ can be observed

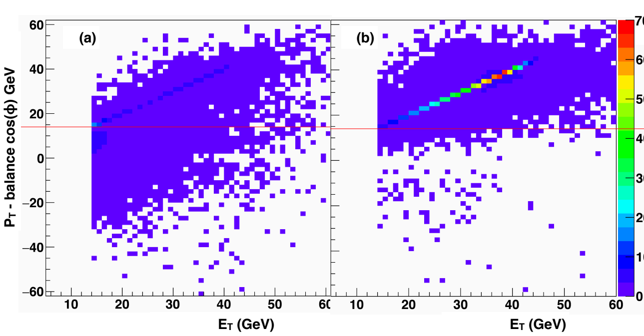

FIG. 2. Signed p_T-balance vs E_T^e for data (a) and $W \to e\nu$ MC (b).

in $W^{\pm} \to e^{\pm}\nu$ candidate events, due to undetected neutrinos in the final state. This leads to a large imbalance in the vector p_T sum of all reconstructed final-state objects in W candidate events, which is expressed as $\vec{p}_T^{\,balance}$ in equation 1. Here the jet transverse momentum, $\vec{p}_T^{\,jets}$ is determined using the anti-k_T algorithm [14], by reconstructing the p_T from all reconstructed jets outside a cone of radius of 0.7 in $\eta - \phi$ space which is centered around the candidate lepton. The $\vec{p}_T^{\,e}$ is the p_T of the candidate lepton. A strong correlation is observed between E_T and the scalar quantity, signed p_T balance, which is defined in equation 2. This can be seen clearly in Figure 2 (b) which shows the MC results simulating $W^{\pm} \to e\nu$ decays.

After initially requiring reconstructed TPC tracks to have $p_T > 10$ GeV, candidate tracks are matched to a 2×2 EMC cluster with transverse energy $E_T > 12$ GeV. W candidate events are then isolated using the large opposite missing energy requirement. This is done by requiring that the E_T fraction of the $2\times2/4\times4$ tower clusters is larger than 95%. The final requirement, which is based on the large imbalance in the vector p_T sum mentioned above, is signed-p_T balance to be greater than 14 GeV, which is indicated by the red line in Figure 2 (a). After all the selection cuts have been applied, the characteristic Jacobean peak in the E_T distribution for mid-rapidity $W^{\pm}$ candidate events can be observed near half of the $W^{\pm}$ mass, as shown in Figure 1.

$$\vec{p}_T^{\,balance} = \vec{p}_T^{\,e} + \sum_{\Delta R > 0.7} \vec{p}_T^{\,jets} \tag{1}$$

$$signed\, p_T\, balance = \frac{(\vec{p}_T^{\,e}).\vec{p}_T^{\,balance}}{|\vec{p}_T^{\,e}|} \tag{2}$$

$W^{\pm}$ candidates were charge separated based on $e^{\pm}$ track curvature measured in the TPC. The Charge separated $W^{\pm}$ yields from the 2013 data sets as a function of E_T^e are shown in Figure 3 for different η bins, along with the estimated residual background contributions from $W^{\pm} \to \tau^{\pm}\nu_\tau$, $Z/\gamma^* \to e^+e^-$ electroweak processes and QCD processes. Relatively small electroweak background contributions are estimated from Monte-Carlo (MC) simulation, with PYTHIA 6.422 [17] generated events passing through the STAR GEANT[18] model and embedded in to STAR zero-bias triggered events. The selection process of W candidate event described above is designed to remove significant amount of QCD type background events. However a certain amount of QCD background will still present in the signal region. This contribution originates primarily from events which satisfy candidate $W^{\pm}$ isolation cuts but contain jets fragments which escape the detection outside the STAR acceptance. Two procedures referred as "Second EEMC" and "Data-driven QCD" [19], are used to estimated the background

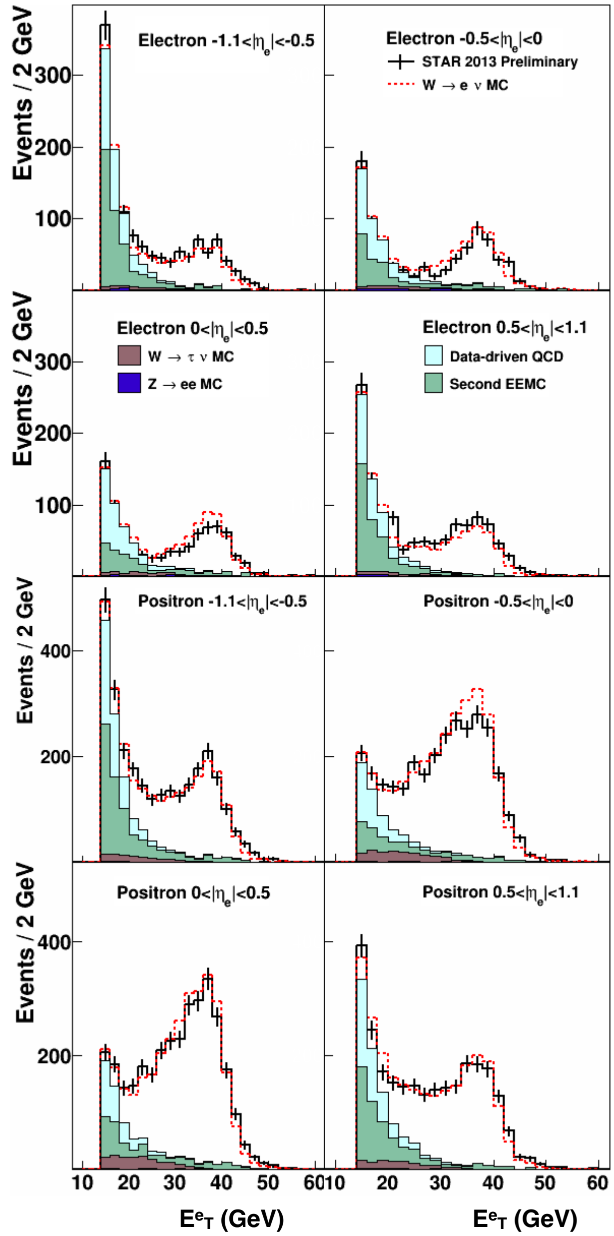

FIG. 3. E_T^e distribution of W^- (top) and W^+ (bottom) candidate events (black), various background contributions and sum of backgrounds and $W \to e\nu$ MC signal (red-dashed).

associated with the acceptance ranges $-2 < \eta < -1.09$ and $|\eta| > 2$ respectively. Second EEMC refers to the $e^{\pm}$ candidate background event that satisfy W isolation requirement which has an opposite-side jet fragment in the range $-2 < \eta < -1.09$, where a fictitious Endcap Electromagnetic calorimeter is present. Therefore this opposite-jet fragment will escape the detection leading the event to satisfy W candidate requirements. The magnitude of this background contribution was estimated by repeating the W signal selection process, but with the real EEMC towers excluded from the isolation ratio, and from the reconstruction of jets summed in the $\vec{p}_T^{\,balance}$

vector, and taking the difference in the E_T^e distributions. The Data-driven QCD refers to the QCD background process that satisfy W candidate selection criteria due to a jet fragments in such a way that it satisfies the isolated $W^{\pm}$ candidate requirements, while all other jets escape detection outside the $\eta < |2|$ acceptance. This component of the background was estimated by determining a data-driven QCD background distribution as a function of E_T^e.

III. RESULTS

The $W^{\pm}$ single-spin asymmetries are calculated using the formula as shown in equation 3.

$$A_L = \frac{1}{\beta}\frac{2}{P_1+P_2}\frac{R_{++}N_{++}-R_{--}N_{--}}{\Sigma R_i N_i} - \frac{\alpha}{\beta} \tag{3}$$

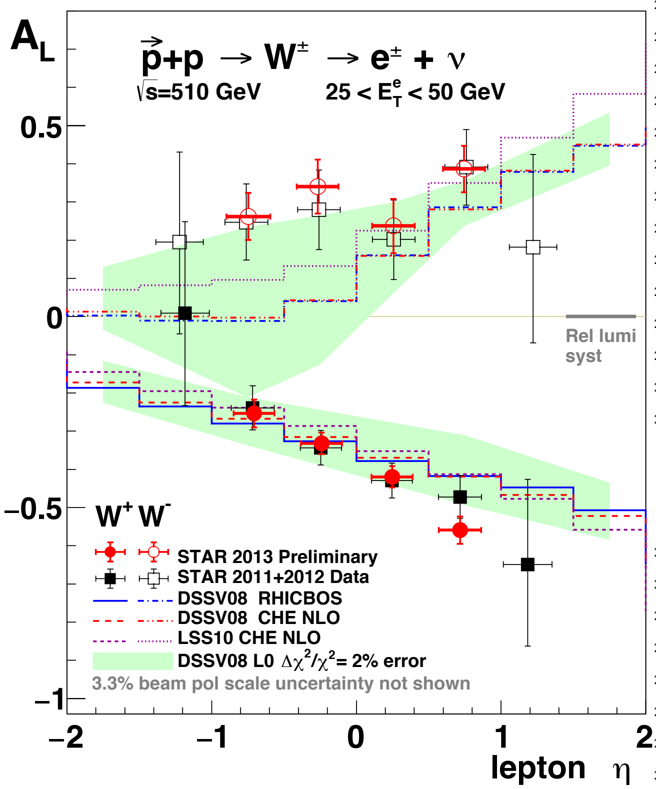

FIG. 4. Longitudinal single-spin asymmetries for $W^{\pm}$ production as a function of lepton pseudorapidity, η_e in comparison to theory predictions

Here, N_i is the reconstructed W yields in each spin configuration corresponds to $++, +-, -+ and --$ of the two collided proton beams, R_i is the relative luminosity of each spin state, P_1 and P_2 are beam polarizations values of each beam, and α and β are polarized and unpolarized background corrections respectively, which are calculated independently for W^+ and W^-. The STAR 2012 published $W^{\pm}$ single-spin asymmetry results (open and closed black square) measured for $e^{\pm}$ are shown in Figure 4 along with recently released STAR 2013 preliminary results (open and closed red circle) as the function of decay $e^{\pm}$ pseudorapidity, η_e in comparison to theoretical predictions based on DSSV08 [20] and LSS10 [21] helicity-dependent PDF sets, using both CHE (next-to-leading order) [14] and RHICBOS (fully resummed) frameworks [22]. The new 2013 preliminary results consist with published 2012 results which measured larger $A_L^{W^-}$ than the central value of the theoretical predictions. The enhancement at large negative η_e, in particular is sensitive to the polarized anti u quark distribution, $\Delta\bar{u}$. $A_L^{W^+}$ is negative as expected and consistent with theoretical predictions. The total uncertainties in both results are completely statistical driven while systematic uncertainties are well under control. The systematic of new 2013 results are on the same order of published 2012 results despite significant enhancement in luminosity in RHIC 2013 running in comparison to previous years. The uncertainty of new 2013 preliminary results is reduced by 40% in comparison to published results making new results as the most precise measurement in the world to the date. The STAR 2012 preliminary $A_L^{W^{\pm}}$ results [4] are included in the DSSV++ global analysis [23] from the DSSV group and recent NNPDF [24] global analysis. Both analyses show that the STAR W A_L results provide a significant constraint on $\Delta\bar{u}$ and $\Delta\bar{d}$ quark polarizations. We expect new STAR 2013 preliminary results to further constrain anti u ($\Delta\bar{u}$) and anti d ($\Delta\bar{d}$) quark polarizations.

The charged W cross section ratio can be measured experimentally as

$$\frac{\sigma_{W^+}}{\sigma_{W^-}} = \frac{N_i^+ - N_B^+}{N_i^- - N_B^-}\frac{\varepsilon^-}{\varepsilon^+} \tag{4}$$

where $\pm$ corresponds to positively or negatively charged lepton, N_i are reconstructed $W^{\pm}$ yields from decay $e^{\pm}$, N_B are estimated background yields and ε is the efficiency at which W events are detected. The detection efficiencies which account for all cut and detector efficiencies are calculated using Monte Carlo based on Pythia 6.4.22 and GEANT simulations. However there was only a small ($\sim 1-2\%$) charge dependence measured between the W^+ and W^- efficiencies leading to a negligible contribution to the charged W cross section ratio. Figure 5(6) shows the charged W cross section ratio for the combined 2011 and 2012 runs, computed using equation 4 as a function of the electron pseudo-rapidity η_e (W boson rapidity, y_W). More information on how the W boson kinematics were reconstructed can be found in [29].

The error bar on the data points represents the statistical uncertainty, while the shaded boxes correspond to the systematic uncertainty. The yellow band and colored curves serve as a comparison to different PDF sets [25][26] and theory frame works [27][28]. The systematic

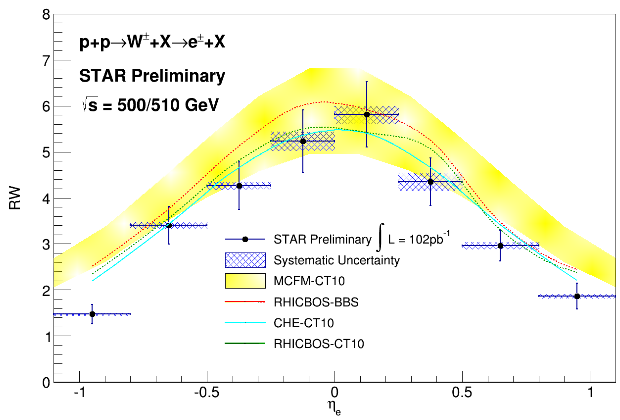

FIG. 5. W^+/W^- cross section ratio as a function of electron pseudo-rapidity.

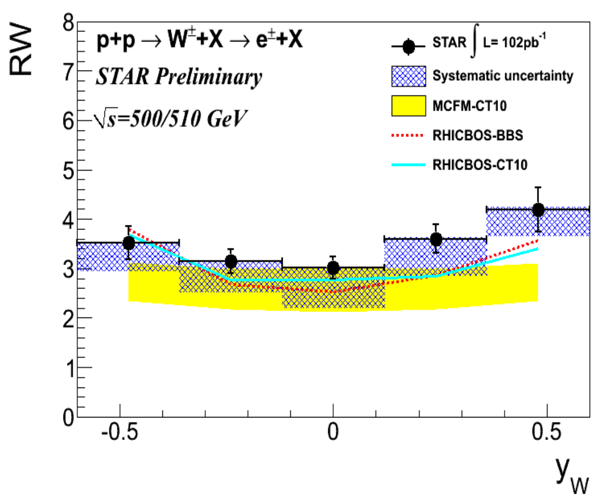

FIG. 6. W^+/W^- cross section ratio as a function of W boson rapidity

uncertainties for the charged W cross section ratios as a function of η_e are well under control and are dominated by the statistical precision similar to the asymmetry analysis. Further studies into the newly established W boson reconstruction process[29] should reduce the systematic uncertainties on the $W^{\pm}$ cross-section ratio dependence on the boson kinematics.

IV. SUMMARY AND OUTLOOK

We present the STAR 2013 preliminary results of measurements of single spin asymmetries for $W^{\pm}$ boson production in longitudinally polarized p+p collisions and STAR 2011+2012 W cross section ratio W^+/W^-, at $\sqrt{s} = 510$ GeV. The new 2013 $A_L^{W^-}$ results are consistent with STAR published 2012 $A_L^{W^-}$ results, further confirming the measured large W^- asymmetry compared to the theoretical prediction indicating a large anti u quark polarization. Furthermore, the uncertainty of new 2013 results is reduced by 40% in comparison to published results making the STAR 2013 preliminary results the most precise measurements of $A_L^{W^-}$ in the world up to date. The uncertainties are purely statistical driven while systematics are well under control. With the reduced uncertainty, we expect our new results to further constrain the antiquark helicity distribution functions. Analysis is ongoing to measure the asymmetry in the forward rapidity region from $1 < \eta < 1.4$ using STAR EEMC subsystem and further extend using STAR Forward Gem Tracker (FGT) which covers the acceptance between $1 < \eta < 2$. This enhances the sensitivity to $\bar{u}$ and $\bar{d}$ quark polarizations. We expect to include these measurements in the publication from STAR 2013 data. STAR has also measured and presented charged W cross section ratios from combined 2011 and 2012 proton-proton STAR data at $\sqrt{s} = 500$ and 510 GeV. The inclusion of this data into global PDF analysis should help constrain the sea quark distributions and provide additional insight into the $\bar{d}/\bar{u}$ ratio at relatively higher Bjorken-x values where the behavior of $\bar{d}/\bar{u}$ is not clearly understand yet.

* devika@temple.edu

[1] J. R Ellis and R. L. Jaffe, A Sum Rule for Deep Inelastic Electroproduction from Polarized Protons, Phys. Rev. **D9**, 1444 (1974).

[2] European Muon Collaboration, J. Ashman *et al.*, Phys. Rev. Lett. **B206**, 364 (1988).

[3] R. Jaffe and A. Manohar, The G(1) Problem: Fact and Fantasy on the Spin of the Proton, Nucl. Phys. **B337**, 509 (1990), revised version.

[4] D. de Florian, R. Sassor, M. Stratmann, and W. Vogelsang, Extraction of Spin-Dependent Parton Densities and Their Uncertainties, Phys. Rev. **D80**, 034030 (2009).

[5] A. Airapetian et al. (HERMES Collaboration), Phys. Rev. **D71**, 012003 (2005).

[6] M. G. Alekseev et al. [COMPASS Collaboration], Phys. Lett. **B680**, 217 (2009).

[7] M. G. Alekseev et al. [COMPASS Collaboration], Phys. Lett. **B693**, 227 (2010).

[8] D. de Florian, R. Sassot, and M. Stratmann, Phys. Rev. **D75**, 114010 (2007); **D76**, 074033 (2007).

[9] R. D. Field and R. P. Feynman, Phys. Rev. D15 (1977) 2590.

[10] G.T. Garvey and J.C. Peng, Flavor asymmetry of light quarks in the nucleon sea, Progress in Particle and Nuclear Physics, **47**, 203-243 (2001)

[11] R. S. Towell et al., Phys. Rev. **D64**, 052002 (2001).

[12] B. Kerns et al. (SeaQuest Collaboration), APS April Meeting, 2016

[13] B. Adeva *et al.*, (Spin Muon Collaboration), Polarized quark distributions in the nucleon from semi inclusive spin asymmtries, Phys. Lett. **B420**, 180 (1998).

[14] D. de Florian and W. Vogelsang, Helicity parton distributions from spin asymmtries in W-boson production at

RHIC, Phys. Rev. **D81**, 094020 (2010).

[15] STAR Collaboration, L. Adamczyk *et al.*, Phys. Rev. Lett. **113**, 072301 (2014).

[16] K.H. Ackermann et al., Nucl. Instrum. Meth. **A 499**, 624 (2003)

[17] T. Sjostrand, S.Mrenna, and P.Z. Skands, PYTHIA 6.4 Physics and Manual, JHEP **05**, 026 (2006).

[18] R. Brun *et al.*, GEANT: Simulation Program for Particle Physics Experiments. User Guide and Reference Manual, CERN-DD-78-2-REV (1978).

[19] STAR Collaboration, L. Adamczyk *et al.*, Phys. Rev. **D85**, 092010 (2012).

[20] D. de Florian, R. Sassor, M. Stratmann, and W. Vogelsang, Phys. Rev. Lett. **101**, 072001 (2008).

[21] E. Leader, A. V. Sidorov, and D. B. Stamenov, Determination of polarized parton densities from a QCD analysis of inclusive and semi-inclusive deep inelastic scattering data, Phys. Rev. **D82**, 114018 (2010).

[22] P. M. Nadolsky and C. Yuan, Nucl. Phys. **B666**, 31 (2003)

[23] E. Aschenauer *et al.*, (2013), arXiv:1304.0079 [nucl-ex].

[24] E.R. Nocera, arXiv:1403:0440 [hep-ph] (2014).

[25] H. L. Lai et al., Phys. Rev. **D82**, 074024 (2010)

[26] C. Bourrely, F. Buccella, and J. Soffer, Eur. Phys. J. C 23, 487 (2002)

[27] J. Campbell, K. Ellis, and C. Williams, *MCFM - Monte Carlo for FeMtobarn Processes*, mcfm.fnal.gov.

[28] P .M. Nadolsky and C.-P. Yuan, Nucl. Phys. **B666**, 3 (2003)

[29] S. Fazio and D. Smirnov (STAR), PoS, DIS2014, 237, (2014)